20th IMEKO TC4 International Symposium and
18th International Workshop on ADC Modelling and Testing
Research on Electric and Electronic Measurement for the Economic Upturn
Benevento, Italy, September 15-17, 2014

The ATLAS Insertable B-Layer (IBL) design, production and integration challenges

J. Bilbao de Mendizabal[1], G. Iacobucci[1], On Behalf of the ATLAS collaboration

[1]*University of Geneva, 24 Quai Ernest-Ansermet Geneva Switzerland, bilbao@cern.ch*

Abstract –

For Run-2 of the LHC a fourth, innermost Pixel Detector layer on a smaller radius beam pipe has been installed in the ATLAS Detector to add redundancy against radiation damage of the current Pixel Detector and to ensure a high quality tracking and b-tagging performance of the Inner Detector over the coming years until the High Luminosity Upgrade

To improve the overall physics performance of the ATLAS detector, a local support structure in carbon fiber has been developed with an overall planarity of $350\mu m$, targeting for a low material budget subdetector with a total radiation length of only 1.5 Xo.

An overview of the new sub-detector called the Insertable B-layer (IBL) will be given, followed by the stave loading process with focus on the stave planarity metrology measurements and module positioning precision. Metrologies surveys on the IBL Support Tube and final package after stave integration will been shown.

I. INTRODUCTION

The ATLAS detector [1], an experiment at the CERN Large Hadron Collider (LHC), is a general purpose particle detector designed to explore new frontiers of particle physics. It is composed of several subdetectors assuring globally the particle reconstruction and identification, making the ATLAS experiment sensitive to a wide range of signatures.

The innermost part of the detector assuring the particle tracking, operational since 2009 with a recorded integrated luminosity of 27 fb^{-1}, is composed of several subsystems with different detector technologies. Closest to the interaction point, three pixel layers assure a high P_T resolution and vertex reconstruction (Pixel Detector [2]), which is essential to cope with the high pileup at LHC ($<\mu>$=19 pileup event/bunch cross at $\sqrt{s} = 8$ TeV).

After successful operation in the last three years, the LHC machine is being upgraded during the 2013-2014 long shutdown to increase the instantaneous luminosity and the collision energy to $\sqrt{s}$ =14 TeV. To ensure the long term physics performance coping with a high occupancy environment and pileup, a detector upgrade has been foreseen [3].

II. THE INSERTABLE B-LAYER

The Insertable B-Layer is a new detector layer at an average radius of only 33 mm from the interaction point and only 9 mm envelope. Integrated into the current Pixel Detector (PD), as its fourth innermost layer and with a higher granularity pixel sensors of 50 x 250 μm, the IBL will maintain the physic performances during Run 1 of the PD.

The IBL is composed of 14 local support structure with integrated cooling circuit (64 cm long, 2 cm wide and tilted in ϕ at 14 degrees), called staves, equipped with 32 front-end per stave and silicon sensors facing the beam pipe cooled down at -35° by the integrated titanium pipe flowed with double phase CO2 [4]. A design with total η coverage up to 3.5 and an overlap between staves of 1.8° to ensure the hermeticity in ϕ (Figure 1).

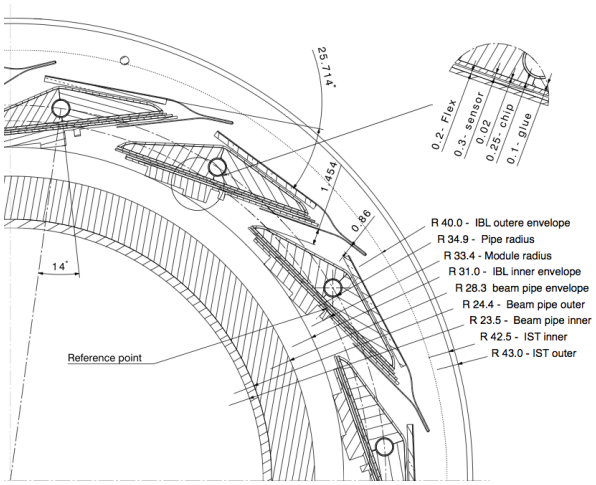

Fig. 1. Transversal cut of the IBL detector and beam pipe. Dimensions in [mm]

III. IBL LOCAL SUPPORT STRUCTURE

The IBL staves (mechanical support and cooling) are composed of an assembly of several carbon fiber parts and titanium pipes as shown in Figure 2.

The laminated carbon fiber, providing stiffness and support to the modules is used for the two central pieces as shown in Figure 2; the top one, called face-plate, devoted to host the modules, and the omega in the bottom.

ISBN-14: 978-92-990073-2-7

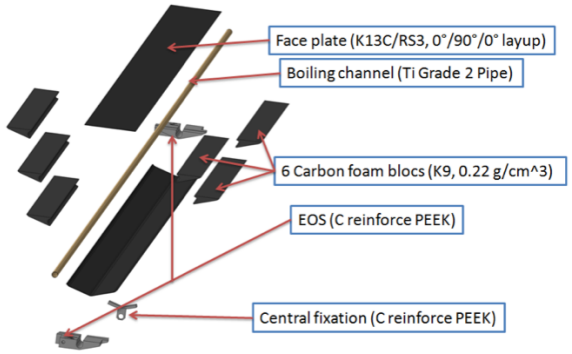

Fig. 2. Bare stave structure.

The stave core filled with carbon foam provides thermal conduction between the cooling pipe and the modules while keeping low the material budget.

Before proceeding with the module loading onto the stave structure, a metrology survey of the bare staves is performed to check that the maximum excursion of the face-plate surface remains under $350\ \mu m$. This planarity value is determinated by the mechanical constrains of the IBL structure during stave integration around the IBL positioning tube (IPT).
A Mitutoyo EURO C 9106 metrology machine was employed, using a 0.997 mm wide probe. The probing head was settle to an angle of $75°$ to decreasing the probing force to $2.5\ g_F$ (with respect to the $8\ g_F$ applied at $0°$). To model the stave surface, 99 points have been probed measuring their coordinates. The arrangement of the 99 points and the orientation of the axes are shown in Figure 3.

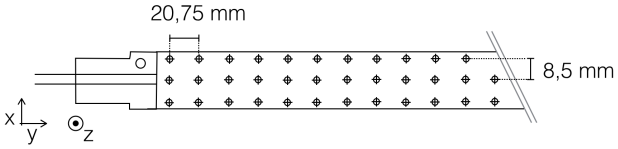

Fig. 3. Schematic view of the stave showing the metrology points location and reference axes. 99 probing points are organized in 3 lines $8.5\ mm$ *spaced. The step of the points in the same line is* $20.75\ mm$.

The planarity results of production staves (before and after bare stave thermal cycling[1]) are summarised on table 2, showing that all production staves were fulfilling IBL planarity specification before module loading.

[1]Consisting of ten cycles cycled from $+40°C$ to $-40°C$ during thirty minutes at each step.

IV. MODULE LOADING ONTO THE STAVES

After the module selection, modules were loaded onto qualified staves. As a first step, the stave were aligned with respect to the loading tool (Figure 4), which provides the reference points and support for all the loading tools while protecting the Omega. Although the stave handling frame provides a good reference alignment of the stave with respect to the loading tools, an additional fine adjustment is performed thanks to two micrometer screws and a metrology measurement between the stave face-plate edge and the loading tool reference points.

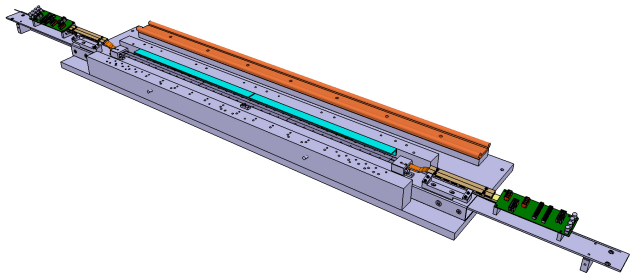

Fig. 4. 3D model of a stave and its handling frame positioned on the loading tool.

Once the stave was aligned with respect to the loading tools, modules were loaded following the protocol as described in [5]. Modules position after loading were checked in z by probing the module at 4 different locations while an optical recognition of the modules fiducial marks was performed to obtain the x and y module's coordinates.

Error distributions of the module loading position are shown in Figure 5 for the x and y axis showing a module loading positioning precision of $50\ \mu m$ for double chip modules in both axes and $56\ \mu m$ in x and $33\ \mu m$ in y for single chip modules.

V. STAVE QA AND RANKING

All produced staves went through an exhaustive quality assurance where all front-end functionalities and sensor integrity where tested at ambient (20°C) and operational temperature (-30°C) [6].

Although all front-end were functional, several pixels were classified as "bad pixels" in the following main categories: defects pertaining to the front-end, sensor or bump bonding. As shown on Table 1 all failures can be classified exclusively from the QA testing, were detailed criteria and test used for identification are specified.

The selection of the 14 staves to integrate around the IPT, among the 18 qualified staves, was performed thanks to the following scoring algorithm:

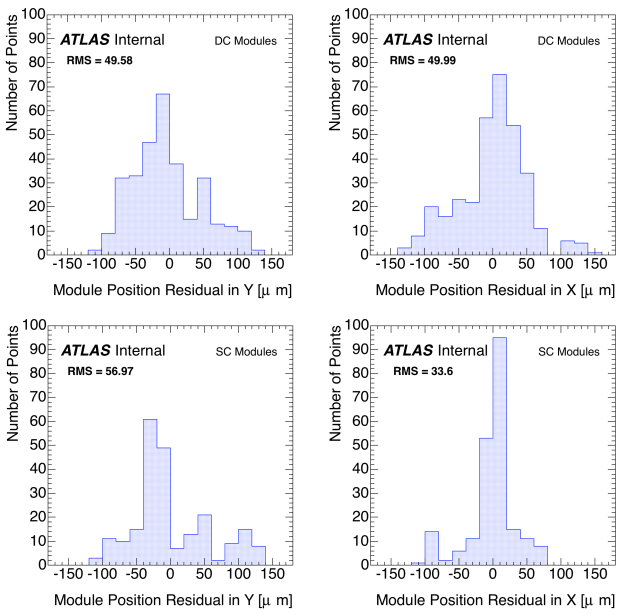

Fig. 5. Residual values of the modules fiducial marks with respect to their nominal position for double chips (DC) and single chips (SC) in x and y directions, where the y axis is along the beam direction.

Failure Name	Scan Type	Criteria
Digital Dead	Digital Scan	Occupancy $< 1\%$ of injections
Digital Bad	Digital Scan	Occupancy $< 98\%$ or $> 102\%$ of injections
Merged Bump	Analog Scan	Occupancy $< 98\%$ or $> 102\%$ of injections
	Crosstalk Scan	Occupancy $> 80\%$ of 25 ke injections
Analog Dead	Analog Scan	Occupancy $< 1\%$ of injections
Analog Bad	Analog Scan	Occupancy $< 98\%$ or $> 102\%$ of injections
Tuning Failed	Threshold Scan	s-curve fit failed
	ToT Test	ToT response is 0 or 14 BCs
Noisy	Noise Scan	Occupancy $> 10^{-6}$ hits per BC
Disconnected Bump	Source Scan (^{90}Sr)	Occupancy $< 1\%$ of mean Occupancy
High Crosstalk	Crosstalk Scan	Occupancy > 0 with 25 ke injection

Table 1. Classification of pixel failures

.

$$V = \frac{\sum_{i \in \text{ bad pixels}} \cosh^{-1}(\eta_i)}{\sum_{i \in \text{ all pixels}} \cosh^{-1}(\eta_i)} \qquad (1)$$

allowing in a simple way, to take into account the "bad pixels" distributed along the stave, weighed by their geometrical acceptance thanks to the factor $\cosh(\eta_i)^{-1}$ (measured in the η-ϕ coordinate system). Scores of all qualified staves can be seen on Table 2.

VI. THE IPT PREPARATION FOR THE STAVE INTEGRATION

The IBL package composed in its inner most part by the new smaller radius beam pipe and the IPT, has been prepared in parallel to host the IBL staves and services.

With an inner diameter of 58 mm and a length of 6766 mm, the IPT is composed of a 5 carbon fibber layers with a total thickness of 0.325 mm at $\eta < 3.5$ and 7 layers (0.455 mm) at larger η. Glued to it, the stave rings are a Quasi-isotropic Construction made of BMI resin and carbon fibber assuring the positioning and anchor point of the 14 IBL staves around the IPT.

A metrology survey has been performed to the stave rings before gluing, checking their inner radius, position and respective phase, to prevent any stress to the carbon fibber tube nor the future integrated staves. Circularity of each stave ring has been checked for two inner radius at different z and deviations of only 250 μm have been found. The phase adjustment between both rings after gluing has been estimated by computing the maximum deviation of the stave planes on the stave ring with respect the respective plane on the other stave ring, maximum measured deviation has been of 32 μm under the 50 μm specifications.

The final spacing between the stave rings after gluing was of 716.200 mm and 716.112 mm at two different ϕ, showing a discrepancy of 200 μm and 116 μm with its nominal position, exceeding the tolerance positioning of 50 μm and showing a non planarity between rings. In order to cope with all non uniformities between the stave rings

Position	Stave	Number of bad pixels	Score	Planarity [μm]
01	ST17	1052	1.01	114
02	ST02	579	0.44	205
03	ST19	971	1.13	266
04	ST09	1110	1.00	229
05	ST18	1266	0.94	336
06	ST04	799	0.69	235
07	ST13	718	0.56	224
08	ST10	646	0.62	243
09	ST11	565	0.58	298
10	ST12	542	0.62	314
11	ST16	879	0.82	329
12	ST06	734	0.79	290
13	ST15	864	0.84	325
14	ST05	601	0.68	189
n/a	ST01	1011	1.04	224
n/a	ST03	1235	2.48	223
n/a	ST14	1877	1.11	218
n/a	ST20	2139	2.01	237

Table 2. Ranking and loading order overview of the 14 IBL staves. The position is sequential around the beam pipe. The cooling pipe of the stave in position 01 is at $\phi = -6.1°$, subsequent staves are displaced by $25.7°$ in ϕ. The score is determined by the number of bad pixels, each of which is weighted according to the position on a stave. A lower score thus translates into a higher quality stave. The planarity shows the difference between the minimum and maximum height of a stave. For completeness, the bottom four lines show numbers for the staves that were not chosen for installation. For the stave loading around the beam pipe, not only this score but a uniform $\eta - \phi$ bad pixel distribution and engineering constraints are also taken into account.

and any CT mismatching, the staves end blocks have been design asymmetrically as shown in Figure 6 allowing a dynamic mechanical contingency of 1 mm.

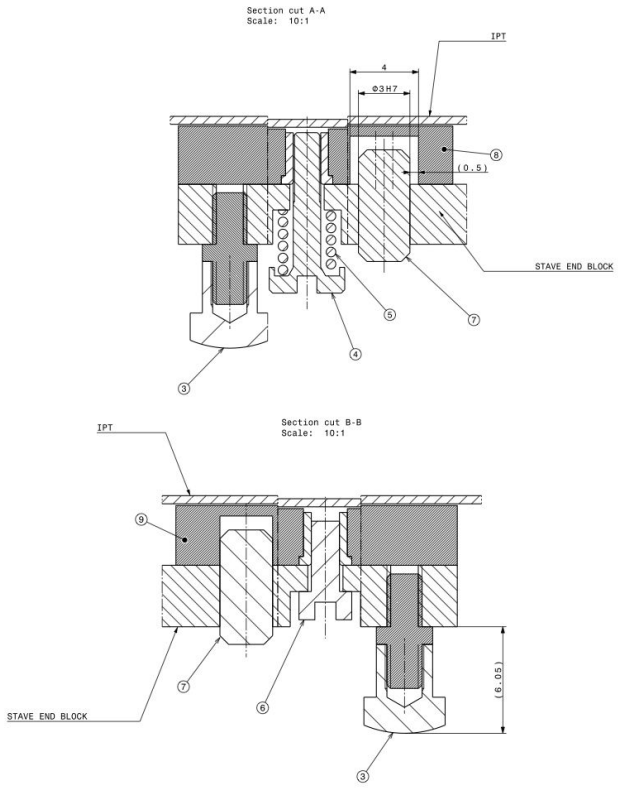

Fig. 6. Transversal cut of the stave end-block showing the anchor sister to the IPT. On top the, A-side is represented showing the pusher (7) with the 1mm contingency. C-side is represented in the bottom showing no contingency and so providing the positioning reference.

VII. CONCLUSION

The IBL detector here introduced, has been successfully assembly and integrated during the 2013-2014 LHC long shutdown after two years of preparation and construction. A very demanding project in detector performances and not only due to its new mechanical design. Metrology surveys over all the process had verify the fulfilment of the mechanical constrains, leading to an smooth detector integration. A great mechanical and physics success with the final insertion of the IBL in the cavern, equipping the ATLAS detector with a fourth pixel layer.

REFERENCES

[1] ATLAS Collaboration, The ATLAS Experiment at the CERN Large Hadron Collider, JINST 3 S08003 229 (2008)

[2] G. Aad et al., ATLAS Pixel Detector Electronics and Sensors, JINST 3 P07007 (2008)

[3] M. Garcia-Sciveres, ATLAS Experiment Pixel Detector Upgrades, arXiv:1109.4662 [physics.ins-det]. Proceedings of Meeting of the Division of Particles and Fields of the American Physical Society, DFF 2011, September 2011

[4] ATLAS Collaboration, ATLAS Insertable B-Layer Technical Design Report, ATLAS-TDR-19

[5] ATLAS Collaboration, IBL Module Loading onto Stave and Quality Check, Internal note

[6] ATLAS IBL Collaboration, ATLAS Pixel IBL: Stave Quality Assurance, ATL-COM-INDET-2014-017